Effects of Peptide Immobilization Sites on the Structure and Activity of Surface-Tethered Antimicrobial Peptides

ARTICLE *in* THE JOURNAL OF PHYSICAL CHEMISTRY C · MARCH 2015

Impact Factor: 4.77 · DOI: 10.1021/jp5125487

THE JOURNAL OF PHYSICAL CHEMISTRY C

Article

pubs.acs.org/JPCC

Effects of Peptide Immobilization Sites on the Structure and Activity of Surface-Tethered Antimicrobial Peptides

Yaoxin Li,[†] Shuai Wei,[‡] Jianfeng Wu,[§] Joshua Jasensky,[‡] Chuanwu Xi,[§] Honglin Li,[⊥] Yanmei Xu,[⊥] Qian Wang,[⊥] E. Neil G. Marsh,[†,‡,∥] Charles L. Brooks, III,[†,‡] and Zhan Chen*[,†,‡]

[†]Departments of Chemistry, [‡]Biophysics, [§]Environmental Health Sciences, and [∥]Biological Chemistry, University of Michigan, Ann Arbor, Michigan 48109, United States

[⊥]Department of Chemistry and Biochemistry, University of South Carolina, Columbia, South Carolina 29208, United States

Supporting Information

ABSTRACT: Antimicrobial peptides, because of their unique structural and chemical properties, hold a promising future for the development of a new class of bacterial-resistant antibiotics, effective antimicrobial coatings, and high performance biosensors. To understand the structure/function relationship of surface-bound peptides as they relate to such applications, sum frequency generation (SFG) vibrational spectroscopy, coarse grained molecular dynamics simulations, and antimicrobial activity tests were used to characterize both surface peptide structural information and peptide activity. Results from MSI-78, an antimicrobial peptide, chemically immobilized via the N- (nMSI-78) or C-terminus (MSI-78n), demonstrate that the attachment site influences the structure and behavior of surface-bound peptides. Although both immobilized peptides adopt an α-helical structure in aqueous buffer, nMSI-78 stands up and MSI-78n lies down on the surface, as indicated by both SFG and MD simulations. Antimicrobial activity tests indicated that peptides that stand up interact with bacterial cells much quicker than peptides that lie down. We believe that this study provides fundamental insights into how to rationally engineer peptides and substrate surfaces to produce optimized abiotic/biotic interfaces for antimicrobial applications and beyond.

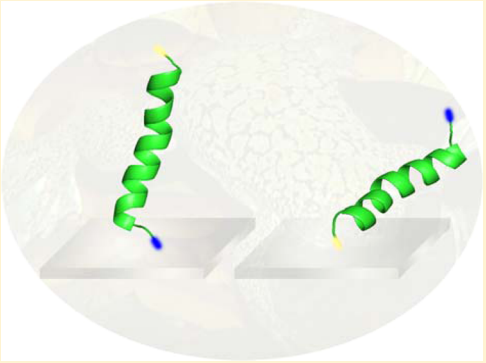

1. INTRODUCTION

Infection is not only the most common problem caused by implanted or indwelling medical devices, but it can be life-threatening to patients.[1] On average, every person in modern society will have a medical implantation at least once in his/her lifetime.[2] Therefore, such infections have huge impact and should either be minimized or prevented entirely. Infections resulting from these indwelling or implanted devices occur because bacterial adhesion, growth, and proliferation lead to biofilm formation on the surfaces of these medical devices (such as urinary or venous catheters, contact lenses, orthopedic implants and stents, or even joint replacement and organ substitution).[3−10] The development of antimicrobial surfaces that can resist biofilm formation or kill bacteria adhered to surfaces represents an important approach to the prevention of bacterial adhesion and proliferation on the surfaces of medical implants.

Antibiotics have been widely used to treat infectious diseases over the past decades, and as a result antibiotic resistance has been developed by many bacteria to the point of becoming a major clinical concern.[11] In addition to conventional antibiotics, many other antibacterial agents have been introduced and extensively studied, including polymers, quaternary ammonium salts, silver nanoparticles, and titanium compounds.[12−15] Although each are effective as an antibacterial treatment, they all possess undesirable side effects, such as high cytotoxicity, short-term bacterial protection, and hypersensitivity.[16] Antimicrobial peptides (AMPs) provide attractive alternative for developing new antibiotics and making antimicrobial coatings.[17−23] AMPs are naturally occurring amphipathic peptides that can selectively target bacteria, fungi, and even human cancer cells through disruption of the cellular membrane.[18,24] AMPs exhibit many desirable properties such as broad spectrum activity, high structural stability, low toxicity for healthy mammalian cells, and low susceptibility to bacterial resistance.[17−19]

The first and most widely studied antimicrobial peptides are peptides in magainin family, which was first isolated from the frog *Xenopus laevis* skin.[25,26] Our studies focus on MSI-78, or pexiganan, an antimicrobial peptide designed by Genaera Corporation, which is a potent synthetic analogue of magainin. It has been reported that MSI-78 adopts an α-helical structure on association with the cell membrane and a random coil structure in aqueous buffer solutions.[27,28] Its short sequence and α-helical structure make it a good choice for structural characterization.

Received: December 16, 2014
Revised: March 5, 2015
Published: March 11, 2015

DOI: 10.1021/jp5125487
J. Phys. Chem. C 2015, 119, 7146−7155

Previous publications have shown that AMPs kill bacteria through the initial electrostatic interactions between the positively charged peptides and the negatively charged bacteria cell membrane, and the later disruption of these membranes due to the amphipathic nature of the peptide.[29] Different killing mechanisms have been proposed, with peptides adopting different orientations associated with cell membranes.[30,31] We have investigated molecular interactions between MSI-78 and various model cell membranes using sum frequency generation (SFG) vibrational spectroscopy as a function of MSI-78 solution concentration.[30] We found that different MSI-78 bulk concentrations in solution led to varied interaction mechanisms with model cell membranes, resulting from different peptide orientations associated with the model cell membranes. Other research groups have also studied membrane disruption of MSI-78 by NMR.[32−37] We note that all previous studies were performed using "free" MSI-78 molecules in bulk solutions.

In this study, we immobilized MSI-78 through different peptide termini onto surfaces to create antimicrobial coatings. We characterized the surface-immobilized MSI-78 structure using SFG, a second-order nonlinear optical spectroscopy that is intrinsically surface sensitive[38,39] and has been applied to examine the secondary structures and orientations of various peptides and proteins adsorbed on surfaces.[40−43] The experimentally deduced MSI-78 structure was further validated using circular dichroic (CD) spectroscopy and coarse-grained molecular dynamics simulations. In addition, we determined the antimicrobial activities of the different peptides to correlate the deduced structural information with the biological efficacy of the AMPs with the hope of understanding the structure−function relationship of surface immobilized AMPs.

2. MATERIALS AND METHODS

All chemicals and solvents were purchased from Sigma-Aldrich (St. Louis, MO) and used without further purification unless otherwise stated.

2.1. Surface Functionalization and SAM Preparation. Right-angle CaF_2 prisms were purchased from Altos Photonics, Inc. (Bozeman, MT). The CaF_2 prisms were soaked in toluene for 24 h and then sonicated in 1% Contrex AP solution from Decon Laboratories (King of Prussia, PA) for 10 min. After that, the prisms were thoroughly rinsed with deionized water (18.2 MΩ cm) and dried under N_2 and then treated with O_2 plasma in a plasma cleaner (Glen 1000P) for 30 s immediately before being coated with SiO_2. A layer of 100 nm of SiO_2 was deposited onto the cleaned CaF_2 prism by an electron-beam deposition process using an SJ-26 evaporator system at a pressure below 10^{-5} Torr with a deposition rate of 5 Å/s. The SiO_2-coated CaF_2 prisms were cleaned under O_2 plasma (PE-25-JW) for 3 min and then were immediately placed into the freshly prepared 1.0 mM alkyne-EG4-silane (Figure 1a) in anhydrous toluene for 24 h at room temperature. The functionalized prisms were then rinsed with copious toluene and methanol and were then dried under nitrogen.

2.2. (-N_3) MSI-78 Surface Immobilization. MSI-78 is a 22-residue antimicrobial peptide with the amino acid sequence: GIGKFLKKAKKFGKAFVKILKK-NH_2. C-terminal amidation of MSI-78 was reported to increase peptide activity.[33] Azido mutated MSI-78 was synthesized using the solid phase Fmoc method with one azido-lysine added to the N-terminus (nMSI-78) or C-terminus (MSI-78n) of MSI-78. The nMSI-78 and MSI-78n sequences are shown in Table 1. Peptide stock solutions were prepared by dissolving 2.0 mg of peptide powder into 8.0 mL of Millipore deionized water (18.2 MΩ cm) and stored in a −30 °C freezer.

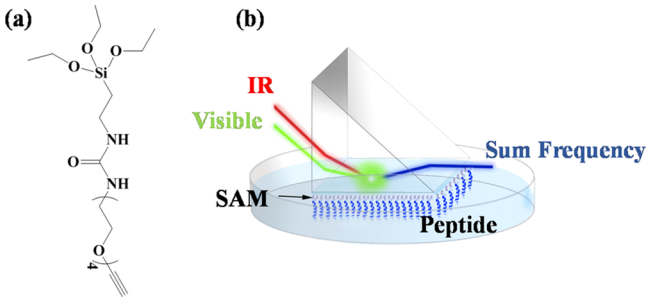

Figure 1. (a) Molecular formula of alkyne-terminated silane. (b) SFG experimental geometry (near-total-reflection geometry) to study immobilized peptide on a right angle CaF_2 prism in contact with phosphate buffer.

Table 1. Amino Acid Sequence of Wild-Type MSI-78, nMSI-78, and MSI-78n

ID	sequence
MSI-78	GIGKFLKKAKKFGKAFVKILKK-NH_2
nMSI-78	(-N_3)KGIGKFLKKAKKFGKAFVKILKK-NH_2
MSI-78n	GIGKFLKKAKKFGKAFVKILKKK(-N_3)-NH_2

The functionalized prisms were placed into a phosphate buffer solution (pH 8.0, ionic strength 5.0 mM) containing nMSI-78 or MSI-78n (9.5 μM), sodium ascorbate (0.2 M), and copper sulfate (0.5 mM) and reacted overnight. The prisms were first rinsed with phosphate buffer containing EDTA to remove any residue copper ion. Then they were rinsed with phosphate buffer and 1.0 mM sodium dodecyl sulfate (SDS) to wash away physically adsorbed peptides, followed by several additional phosphate buffer washes.

2.3. Circular Dichroism Measurement (CD). The CD spectra of free MSI-78 in solution and immobilized MSI-78 on surfaces were collected with a J-815 CD spectrometer (Jasco Inc., Japan) using a continuous scanning mode at room temperature. All the spectra were scanned between 190 and 240 nm at a 1 nm resolution, 20 nm min^{-1} scan rate, and averaged by five successive scans for each sample. Quartz slides were used as substrates for CD studies to immobilize peptides using the same method described in sections 2.1 and 2.2.

2.4. SFG Measurement. The SFG setup used in this study was purchased from EKSPLA. The details regarding SFG theories and measurements have been described previously and will not be reiterated here.[44−61] SFG is a second-order nonlinear optical technique and is intrinsically sensitive to surfaces and interfaces. In our experimental setup, two laser beams (one 532 nm visible laser beam and one frequency tunable IR beam) pass through one surface of a right angle CaF_2 prism and then overlap spatially and temporally at the other surface (shown in Figure 1b). The incident angles of the 532 nm and IR beams in the SFG setup are 58° and 55° relative to the surface normal respectively before going through the prism. SFG spectra with different polarization combinations of the input and generated signal beams including ssp (s-polarized output SFG signal, s-polarized input visible beam, and p-polarized input IR beam) and ppp were collected using the near total internal reflection geometry.[62]

DOI: 10.1021/jp5125487
J. Phys. Chem. C 2015, 119, 7146−7155

For an α-helical structure, the amide I signal is centered at about 1650 cm^{-1}.[63] The orientation of an α helix can be deduced from the measured ratio of the effective second-order nonlinear optical susceptibility tensor components detected in ssp and ppp polarizations.[40,43] This method has been applied to deduce orientation of peptides associated with lipid bilayers.[30,64]

SFG spectra are fitted using the following equation as previously reported:[43]

$$\chi^{(2)}_{\text{eff}}(W) = \chi^{(2)}_{\text{NR}} + \sum_q \frac{A_q}{\omega - \omega_q + i\Gamma_q} \quad (1)$$

where ω is the frequency of the IR beam, A_q is the amplitude of the vibrational mode, and Γ_q is the damping coefficient of the qth vibrational mode.

2.5. Coarse-Grained Molecular Dynamics Simulations on Immobilized MSI-78. A previously developed coarse-grained surface force field is used in this work to study the peptide and surface interaction.[65] This model was developed based on the Karanicolas and Brooks' (KB) Go-like protein model[66,67] and was well parametrized based on a set of benchmark experimental data for protein adsorption free energies onto SAM surfaces.[68] The KB protein model is used because it has been shown to be able to consistently reproduce protein folding free energy surfaces and folding mechanisms. Using the formation of native contacts defined in KB protein model, a five-term potential was used to describe the interaction between each residue and a SAM surface (as shown below in eq 2). The first three terms describe the adsorption well and the energy barrier, which are general for any residue and surface type. The last two terms are used to delineate the hydrophobicity of each residue and surface.

$$V_{\text{surface}} = \sum_i^N \left\{ \pi\rho\sigma_i^3\varepsilon_i \left[\theta_1 \left(\frac{\sigma_i}{z_{is}}\right)^9 - \theta_2 \left(\frac{\sigma_i}{z_{is}}\right)^7 + \theta_3 \left(\frac{\sigma_i}{z_{is}}\right)^3 - (\theta_s(\chi_s - 4.5) + \theta_p\chi_p)\left(\frac{\sigma_i}{z_{is}}\right)^3 \right] \right\} \quad (2)$$

All θ's are parameters that were optimized as shown in Table 2. An alkyne surface is hydrophobic with χ_s set to be 4.5.[65] The values of χ_p are hydropathy indices of residues that can be found in many biochemistry textbooks.[69] The bond between the alkyne surface and the lysine side chain was simulated through the addition of a harmonic restraint tethering the terminal residue of the peptide to the surface and represented by an interaction potential of the following form:

$$U_{\text{restraint}} = \frac{1}{2}k_r(r - r_{\text{eq}})^2 \quad (3)$$

where k_r = 10 kcal/mol is the parameter describing the strength of the restraint and r is the distance of the tethering site from the origin of the surface (0, 0, 0), and r_{eq} = 9.2 Å is the equilibrium distance from the tethering site to the surface origin. The tethering length was used to approximate the distance between the alkyne surface and the C_α of the lysine residue at the tethering site.

2.6. Antimicrobial Activity Test of the Immobilized Peptide. Quartz slides were used to grow SAMs and immobilize peptides in the antimicrobial activity test (instead of prisms used in SFG) using the same method presented above.

A LIVE/DEAD BacLight Bacterial Viability kit (L-7007, Invitrogen, Carlsbad, CA) was used to determine bacterial cell viability. A solution of the mixed SYTO 9 and propidium iodide (PI) dyes was prepared according to the manufacturer's instruction. *Escherichia coli* ATCC 25922 or *Staphylococcus aureus* ATCC 25923 was grown in Luria–Bertani (LB) broth (3 mL, pH 7.2) at 37 °C overnight. The overnight grown bacterial culture was diluted with fresh LB medium to a concentration around 10^8 CFU/mL. A 5.0 μL sample of diluted bacterial culture was mixed with the fluorescent dyes (5.0 μL); the mixture was dropped onto a peptide-coated quartz slide or an untreated quartz slide (control), and a glass coverslip (2.5 cm × 2.5 cm) was placed on the droplet. This slide sample was incubated at room temperature in a dark environment for 15 min before being examined using a fluorescence microscope (Olympus IX71, Center Valley, PA) equipped with a fluorescence illumination system (X-Cite 120, EXFO) and appropriate filter sets. Images were randomly acquired on different spots by using an oil immersion 60× objective lens.

Table 2. Parameters for the Surface Model[65]

θ_1	θ_2	θ_3	θ_s	θ_p
0.2340	0.4936	0.1333	0.0067	0.0333

3. RESULTS AND DISCUSSION

3.1. Secondary Structures of (-N_3) MSI-78. The amino acid sequences of the wild-type MSI-78 and terminal azide modified MSI-78s are shown in Table 1. Previous studies indicated that wild-type MSI-78 adopts a random coil conformation in aqueous buffer solution but forms an α-helical

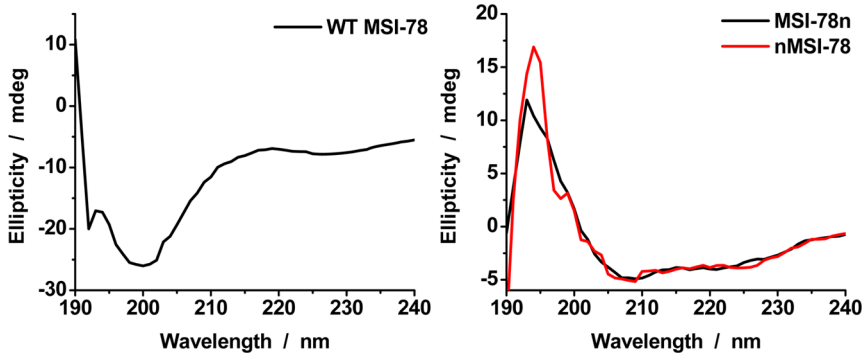

Figure 2. CD spectra of (a) WT MSI-78 in phosphate buffer and (b) surface-immobilized nMSI-78 and MSI-78n in phosphate buffer.

DOI: 10.1021/jp5125487
J. Phys. Chem. C 2015, 119, 7146–7155

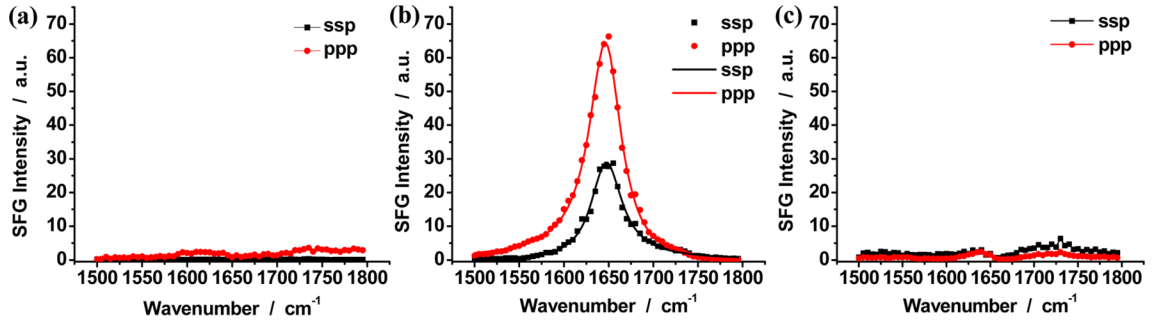

Figure 3. SFG ssp (black square) and ppp (red circle) spectra collected from (a) alkyne-terminated SAM surface; (b) nMSI-78 and (c) MSI-78n immobilized at the alkyne-terminated SAM-phosphate buffer interface.

conformation in the presence of lipid vesicles.[27] The CD spectra of wild-type MSI-78 dissolved in phosphate buffer and azido-derivatives of MSI-78 (nMSI-78 and MSI-78n) after immobilization on surfaces at room temperature are shown in Figure 2. Similar to the wild-type MSI-78, the azido derivatives of MSI-78 adopt a random coil conformation in aqueous buffer solution (not shown). After surface coupling through the reaction of the MSI-78 azido group with the surface alkyne group, the immobilized azido derivatives of MSI-78 exhibited an α-helical conformation, as characterized by the double minima at 207 and 222 nm in the CD spectra (Figure 2b). The helix contents of the surface bound nMSI-78 and MSI-78n are similar at ~84.5% and ~83.7%, as calculated by CDSSTR, SELCON3, and CONTIN.

The CD spectra shown in Figure 2b indicate that a significant conformational change occurred after surface immobilization for both nMSI-78 and MSI-78n. Therefore, it appears that surface tethering stabilizes the α-helical conformation, even in the absence of lipid vesicles or other membrane mimic species, e.g., 2,2,2-trifluoroethanol (TFE).[70] Similar effects have been observed for other peptides upon surface immobilization through cysteine−maleimide coupling.[70−72]

3.2. Orientations of MSI-78 Molecules Surface-Immobilized through N- and C-Termini. After the structures of the immobilized nMSI-78 and MSI-78n were determined to be α-helical using CD, we investigated their surface orientations using SFG. SFG spectra were first recorded from the alkyne-terminated SAM on CaF_2 prism in contact with phosphate buffer in the absence of immobilized peptides (Figure 3a). A small peak around 1620 cm^{-1} was detected in the SFG spectrum, which likely originates from the C═O groups in the silane molecules. Therefore, the alkyne-terminated SAM does not contribute large background SFG signals in the 1500−1800 cm^{-1} wavenumber range that would interfere with the amide I signal that should be centered at ~1650 cm^{-1}.

After overnight reaction of the alkyne SAM with either nMSI-78 or MSI-78n, the SAM surface was rinsed using phosphate buffer containing EDTA, followed by a rinse using SDS to remove physically adsorbed peptides and phosphate buffer. SFG spectra were then collected from each immobilized peptide on SAM in contact with a phosphate buffer solution. An SFG amide I peak centered at ~1650 cm^{-1} was detected (Figure 3b), originating from the α-helical conformation of immobilized nMSI-78. The SFG results agree with the conclusion obtained from the CD spectra shown in Figure 2. Surfaces derivatized with immobilized nMSI-78 were stable when stored in phosphate buffer at room temperature for at least 2 days and when stored frozen at −30 °C for at least 1 month. SFG spectra collected from the stored samples of immobilized nMSI-78 and showed no noticeable change from freshly prepared samples (data not shown).

The SFG ppp and ssp spectra detected from the immobilized nMSI-78 were fitted using a standard SFG spectra fitting method[43] as shown in Figure 3b. The measured χ_{ppp}/χ_{ssp} ratio of the amide I peak at 1650 cm^{-1} is 1.60, which can be used to deduce the orientation of immobilized nMSI-78 and will be discussed further below. We also collected SFG spectra from surface-immobilized MSI-78n, as shown in Figure 3c. Differently from nMSI-78, no discernible SFG signal could be detected under either *ppp* or *ssp* polarization combinations from MSI-78n after surface immobilization. This indicates that either the immobilized peptide molecules have a random coil conformation or that they adopt an α-helical structure but with the helix axis running parallel to the surface. The CD spectra of MSI-78n immobilized on the surface demonstrate that the immobilized MSI-78n molecules *do* adopt an α-helical conformation, implying that the absence of SFG amide I signal is due to a parallel surface orientation of the peptide.

The orientation of a surface-immobilized α-helical peptide can be defined by a tilt angle θ, which represents the angle between the principal axis of the helical peptide and the surface normal. This tilt angle θ can be determined by measuring the χ_{ppp}/χ_{ssp} ratio of the SFG amide I signal of the helix, the details of which have been published previously.[40,43] The dependence of the χ_{ppp}/χ_{ssp} ratio on the helix orientation angle for MSI-78 is plotted in Figure 4. For the surface immobilized nMSI-78, the measured SFG signal strength ratio χ_{ppp}/χ_{ssp} is 1.60 (fitting parameters shown in Table 3). Based on this ratio and the relationship between the χ_{ppp}/χ_{ssp} ratio and the tilt angle shown in Figure 4, the orientation of the surface tethered nMSI-78 is

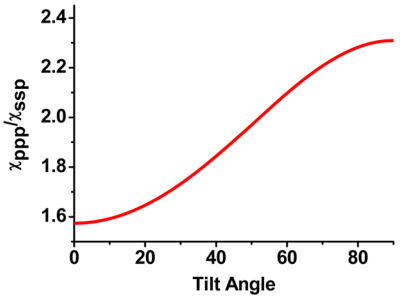

Figure 4. Calculated χ_{ppp}/χ_{ssp} SFG susceptibility tensor component ratio plotted as a function of α-helix orientation angle with a delta distribution.

DOI: 10.1021/jp5125487
J. Phys. Chem. C 2015, 119, 7146−7155

Table 3. SFG Fitting Parameters

system	polarization combination	peak center (cm^{-1})	peak width (cm^{-1})	amplitude
nMSI-78	*ppp*	1650	25.0 ± 0.1	175.4 ± 0.5
	ssp	1650	25.0 ± 0.2	109.6 ± 1.0

~12° relative to the surface normal. Therefore, nMSI-78 is approximately perpendicular to the surface, in striking contrast to MSI-78n, which is approximately parallel to the surface as discussed above.

Previously we investigated the surface orientation of immobilized antimicrobial cecropin P1.[70−72] In that study, cecropin P1 was immobilized onto a SAM surface via cysteine−maleimide coupling rather than the click reaction used here. We found that C-terminus cysteine modified cecropin P1 (CP1c) adopted a perpendicular orientation to the surface whereas the N-terminus cysteine modified cecropin P1 (cCP1) adopted a parallel orientation. Therefore, we believe that the site-dependent changes in structure we observe for peptides immobilized on surfaces is a general phenomenon.

2,2,2-Trifluoroethanol (TFE) has the capability to induce the formation of an α-helical structure of peptides in solution.[70] In this research, SFG spectra were collected from the immobilized nMSI-78 and MSI-78n at the interface between SAM and 50% TFE in phosphate buffer (Figure 5). SFG signals of both immobilized nMSI-78 and MSI-78n increased, indicating that TFE induces a greater helical content for the immobilized peptides. The detection of SFG amide I signal from MSI-78n confirmed the immobilization of MSI-78n on the alkyne-terminated SAM. The SFG spectra in Figure 5 were fitted and the measured χ_{ppp}/χ_{ssp} ratios were deduced to be 1.78 and 2.20, respectively, for nMSI-78 and MSI-78n. From these data the tilt angles for immobilized nMSI-78 and MSI-78n were determined to be ~34° and ~69°, respectively. When the surface is in contact with TFE/phosphate buffer solution, TFE molecules tend to replace the water molecules around the peptides and then interact with the hydrophobic sides of the helices, inducing more α-helical structure formation. Under this condition, the intermolecular and intramolecular interactions are different, which might change the orientation as discussed further below. The SFG signal intensity from nMSI-78 is stronger than MSI-78n. SFG signal intensity is determined by the surface coverage and orientation of a certain functional group. Assuming a similar structure for immobilized MSI-78n and nMSI-78, based on the fitted amplitude and the deduced orientations (fitting parameters shown in Table 4), the coverage of nMSI-78 is about 2 times that of MSI-78n.

Table 4. SFG Fitting Parameters

system	polarization combination	peak center (cm^{-1})	peak width (cm^{-1})	amplitude
nMSI-78	*ppp*	1650	25.0 ± 0.1	284.2 ± 1.1
	ssp	1650	25.0 ± 0.1	159.3 ± 0.7
MSI-78n	*ppp*	1650	25.0 ± 0.3	66.6 ± 0.6
	ssp	1650	25.0 ± 0.5	30.2 ± 0.5

3.3. Coarse-Grained Molecular Dynamics Simulation of Immobilized (-N_3) MSI-78. As discussed above, we previously observed that CP1c and cCP1 immobilized at a maleimide-terminated SAM surface via different termini exhibit different orientations. It was found in these studies that the observed trends from experiment were well reproduced with the simulations, and additionally, the models provided insights into the origin of structural differences resulting from the alternative tethering configurations.[72]

To provide a more detailed understanding of physical origins of different orientations of immobilized nMSI-78 and MSI-78n observed in this research, we performed coarse-grained molecular dynamics simulations. As stated in the method, we use χ_s of 4.5 for the hydrophobic alkyne SAM surface and the tethering length was approximated to be 9.2 Å based on the length of the side chain of the lysine residue. In the simulation, no external force to constrain the helical structure was used other than the native contacts of the initial helical structure which are defined by the Go-like protein model. As shown in Figure 6, the MSI-78 peptide is colored in blue for hydrophilic

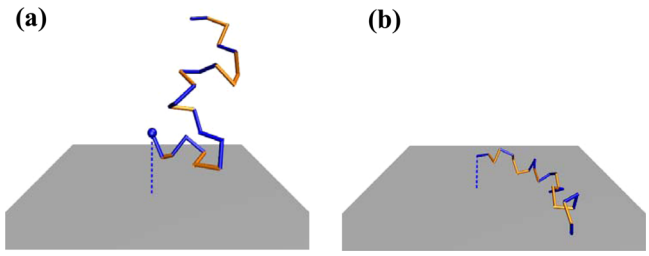

Figure 6. Coarse-grained simulation results of (a) nMSI-78 and (b) MSI-78n immobilized on alkyne-terminated SAMs exposed to phosphate buffer solution. The simulated results well recapitulate the experimentally deduced peptide orientations.

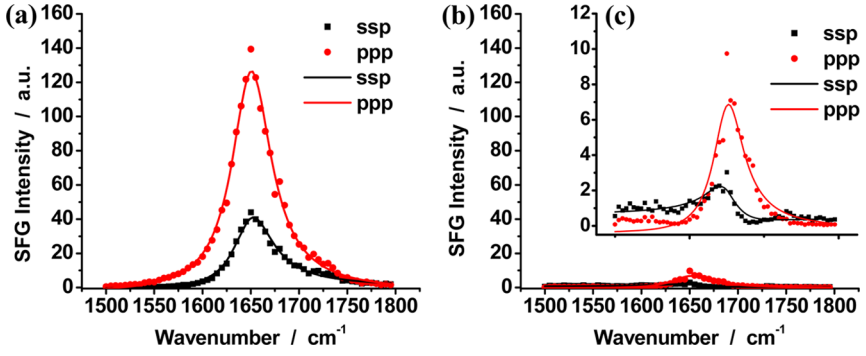

Figure 5. SFG *ssp* (black square) and *ppp* (red circle) spectra collected from (a) nMSI-78; (b) MSI-78n; (c) zoomed in spectra of MSI-78n immobilized on the alkyne-terminated SAMs-50% TFE/phosphate buffer solution interface. The red/black curve is the fitting curve of the experimental data.

DOI: 10.1021/jp5125487
J. Phys. Chem. C 2015, 119, 7146−7155

a) Against *E.coli* by MSI-78n in 30 min

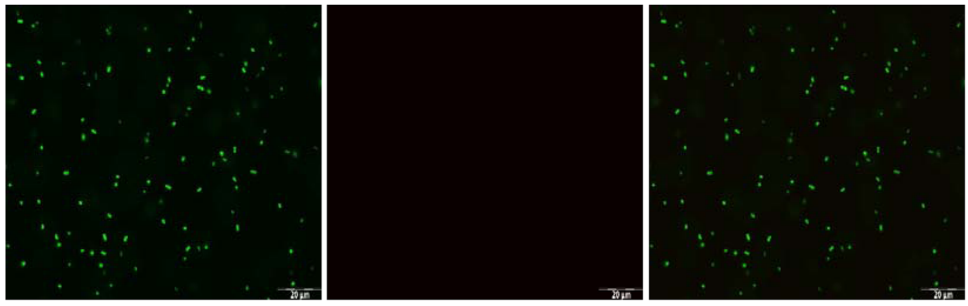

b) Against *E.coli* by MSI-78n in 60 min

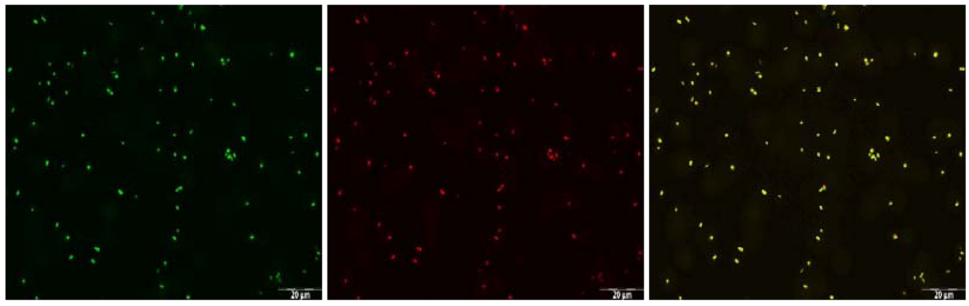

c) Against *E.coli* by nMSI-78 in 30 min

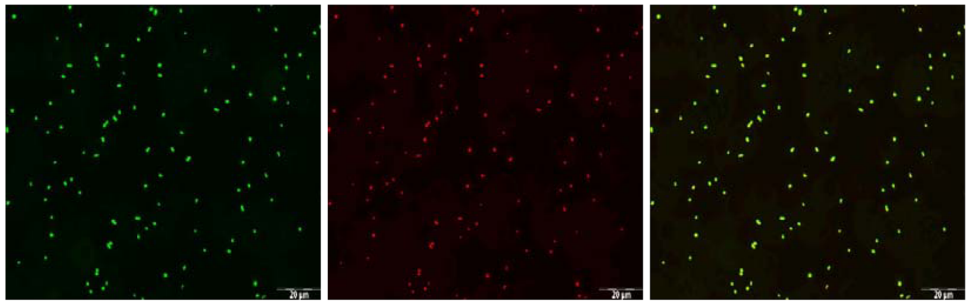

d) Against *E.coli* by nMSI-78 in 60 min

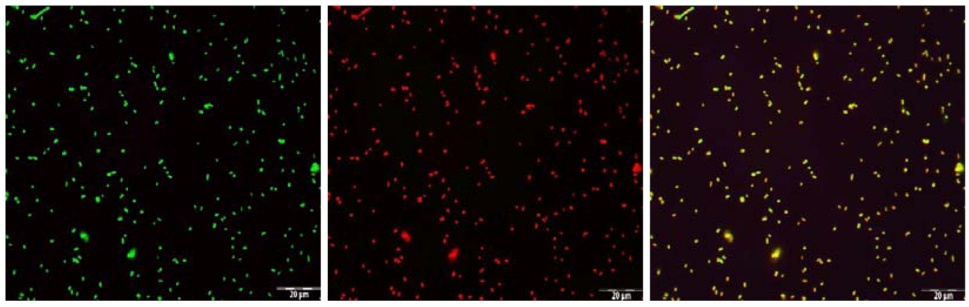

Figure 7. Representative micrographs of antibacterial test results of surface immobilized MSI-78n against *E. coli* for (a) 30 min and (b) 60 min; antibacterial test results of surface immobilized nMSI-78 against *E. coli* for (c) 30 min and (d) 60 min.

residues and orange for hydrophobic residues. Generally, the MSI-78 hydrophobic residues are more likely to be adsorbed onto the alkyne surface. Thus, the orange residues tend to face to the surface. Comparing to CP1,[72] the hydrophobic residues in MSI-78 are more symmetrically distributed with a small cluster of hydrophobic residues gathered near the C-terminus. Furthermore, the lysine (or charged) residues are equally dispersed with the hydrophobic residues throughout the sequence.

As observed in Figure 6b, the hydrophobic residues clustered near the C-terminus of MSI-78n adsorbed to the surface first, forcing the conformation of the entire peptide to lie down. In contrast, as shown in Figure 6a, only several hydrophobic residues of nMSI-78 close to the surface were adsorbed; however, the rest of the peptide was still well accommodated in

DOI: 10.1021/jp5125487
J. Phys. Chem. C 2015, 119, 7146−7155

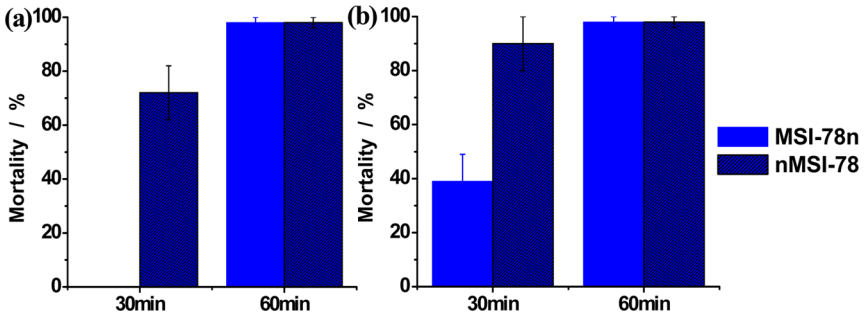

Figure 8. Antimicrobial activities of surface immobilized peptides immobilized against (a) *E. coli* and (b) *S. aureus*. The presented data are the averaged data measured in three spots at each time on the same surface.

the solution and did not lie down on the surface. This result suggests that the N-terminus tethered nMSI-78 peptide on the surface should generate SFG signals due to the standing-up pose, while the C-terminus tethered peptide with a lying-down pose should not. From the above observation, it can be seen that because the hydrophobic segments did not have favorable interactions with water, they liked to be adsorbed to the surface. This was the case for MSI-78n, which adopted a lying-down orientation. Then why did the hydrophobic residues near the C-terminus of the immobilized nMSI-78 remain in the solution instead of being adsorbed to the surface? We believe that this is due to the four lysine residues which are located near the hydrophobic residues close to the C-terminus. When this region of the peptide was far away from the surface (as the case with N-terminus tethered MSI-78), the charged lysine residues preferred to stay in aqueous solution, overcoming the unfavorable interactions between the hydrophobic residues and water, leading the peptide to adopt a tilted orientation relative to the surface and remain solvated in the phosphate buffer. At the same time, it was less probable for the hydrophilic end of nMSI-78 (N-terminus) to interact with the hydrophobic surface. As we observed, nMSI-78 was standing up, only slightly tilting from the surface normal. Therefore, due to the overall effects of the hydrophobic and lysine residues, as the hydrophobic C-terminus of MSI-78 was immobilized, the peptide tended to lie down on the surface, but when the hydrophilic N-terminus was tethered to the surface, MSI-78 stood up on the surface.

As we discussed above, when the aqueous phosphate buffer was replaced by a more hydrophobic TFE−phosphate buffer mixture, the interaction between TFE and peptide should be considered. With a different solvent, the orientation of immobilized MSI-78 peptide here also changed. The immobilized nMSI-78 via the N-terminus tilted more toward the surface—as we observed, the orientation changed from ∼12° to ∼34° relative to the surface normal. With a more hydrophobic solvent, the "free" C-terminus of nMSI-78 is still stable in the TFE−phosphate buffer mixture. However, it becomes easier for the hydrophobic residues at the N-terminus of nMSI-78 to find the hydrophobic alkyne surface. Therefore, nMSI-78 was tilting a bit more in TFE than in water. The opposite effect was observed for MSI-78n. When the phosphate buffer was replaced by a more hydrophobic TFE−buffer mixture, MSI-78n stood up more, as we observed using SFG.

3.4. Antimicrobial Activity Tests of Surface Immobilized MSI-78. We investigated whether the different orientations of immobilized nMSI-78 and MSI-78n result in different antimicrobial activities as well. Antimicrobial activity tests were performed on the immobilized nMSI-78 and MSI-78n against both *Escherichia coli* (*E. coli*) and *Staphylococcus aureus* (*S. aureus*) to examine the relationship between the surface orientation of immobilized MSI-78 and its antimicrobial activity. The bacteria were stained with the Bacterial LIVE/DEAD dyes and characterized by fluorescence microscopy. Figure 7 displays the fluorescence images of live cells (green channel) and dead cells (red channel) on either the nMSI-78 or MSI-78n immobilized surfaces and the merged images. Initially, live bacteria stained with SYTO-9, generating a green fluorescence signal. When the bacteria died or their membranes were compromised, they stained with PI, a red fluorescent dye. Thus, in a merged image damaged or dead cells appear yellow.

The bacterial properties of the nMSI-78 and MSI-78n immobilized surfaces were found to be very different (Figures 7 and 8). Figure 7a shows that the surface with MSI-78n immobilized adsorbs some *E. coli* (green fluorescence signals were observed) after 30 min, but no dead bacteria were observed (no red fluorescence signal was observed). Figure 7b shows that after 60 min the adsorbed bacteria on the surface with immobilized MSI-78n were dead; the red and green fluorescence images overlaid, indicating that all the originally adsorbed bacteria were killed. In contrast, Figure 7c shows that immobilized nMSI-78 killed most *E. coli* cells after only 30 min, with red and green fluorescence signals coinciding. After 60 min, more bacteria were adsorbed onto the surface with immobilized nMSI-78, and again all the adsorbed bacteria were killed. The quantitative results were also shown in Figure 8a. As we discussed above, the immobilized nMSI-78 adopts an α-helical conformation and a "standing up" orientation. Differently, the immobilized MSI-78n lies down. Therefore, very likely peptides with a "standing up" orientation initially have a quicker antimicrobial activity toward *E. coli*.

The initial different orientations of nMSI-78 and MSI-78n likely affect the electrostatic interactions between the negative charged bacterial cell membrane and the cationic peptide, resulting in a change in the activity efficacy of the peptide. According to previous studies,[18,29] for free antimicrobial peptides in solution, as the bacteria attached to peptides, peptide can interact with the lipid bilayers in several different models. In these models, toroidal pore is the accepted mechanism model for MSI-78 in bulk solution.[34] Here the peptides were immobilized on surfaces, and therefore they would unlikely form toroidal pores. Also, to directly interact with the bacterial inner membrane, the peptides need to penetrate through the bacteria outer membrane, which is unlikely for the peptides immobilized on a surface. Therefore, the detailed interaction mechanism between bacteria and surface immobilized antimicrobial peptides is still an open question. Nevertheless, here we showed clearly that the

DOI: 10.1021/jp5125487
J. Phys. Chem. C 2015, 119, 7146−7155

different initial orientations of surface immobilized peptides influenced their antimicrobial activity, which must be due to the differed peptide−bacteria interactions and will be investigated further in the future.

Similar results of the antimicrobial activity against *S. aureus*, Gram-positive bacteria, are shown in Figure 8b. With more negative surface charge,[73] *S. aureus* may have a stronger electrostatic interaction with cationic peptide, resulting in a slightly higher antimicrobial efficacy.

4. CONCLUSION

We have demonstrated that MSI-78 molecules immobilized on a SAM surface via "click" reactions adopt α-helical conformations using a combination of CD and SFG spectroscopies. SFG results indicated that the peptides immobilized through the N- and C-termini adopt different orientations on the surface due to different interactions between the peptides and the hydrophobic surface. SFG results were validated by coarse-grained molecular dynamics simulations. The MSI-78 immobilized through the N-terminus adopts a nearly perpendicular orientation with respect to the surface after covalent attachment to the alkyne-terminated SAM surface. In contrast, the C-terminal-immobilized MSI-78 peptide appears to adopt a parallel orientation with respect to the surface. The antimicrobial activity of the immobilized MSI-78 derivatives was found to be dependent on whether the peptide was tethered through the N- or C-terminus, with nMSI-78 exhibiting significantly better antimicrobial activity than MSI-78n. This study provides fundamental and in-depth insights into understanding the structure−function relationship of immobilized peptides on abiotic surfaces that may aid in the design and development of antimicrobial coatings and devices.

■ ASSOCIATED CONTENT

Supporting Information

Time-dependent native contacts and orientation distributions of N- and C-terminus immobilized MSI-78 obtained from the simulations. This material is available free of charge via the Internet at http://pubs.acs.org.

■ AUTHOR INFORMATION

Corresponding Author

*E-mail: zhanc@umich.edu (Z.C.).

Notes

The authors declare no competing financial interest.

■ ACKNOWLEDGMENTS

This research was supported by the Army Research Office (W911NF-11-1-0251). We thank Dr. Benjamin Buer and Dr. Bishwajit Paul for peptide synthesis, Dr. Yuwei Liu, Dr. Pei Yang, Dr. Bei Ding, Dr. Xiaoxian Zhang, John Myers, and Karthik Pisupati for useful discussions about data analysis, and Lurie Nanofabrication Facility at the University of Michigan for SiO_2 deposition.

■ REFERENCES

(1) Vertes, A.; Hitchins, V.; Phillips, K. S. Analytical Challenges of Microbial Biofilms on Medical Devices. *Anal. Chem.* **2012**, *84*, 3858−3866.

(2) Gristina, A. G. Biomaterial-centered Infection: Microbial Adhesion Versus Tissue Integration. *Science* **1987**, *237*, 1588−1595.

(3) Hall-Stoodley, L.; Costerton, J. W.; Stoodley, P. Bacterial Biofilms: from the Natural Environment to Infectious Diseases. *Nat. Rev. Microbiol.* **2004**, *2*, 95−108.

(4) Nickel, J.; Ruseska, I.; Wright, J.; Costerton, J. Tobramycin Resistance of Pseudomonas Aeruginosa Cells Growing as a Biofilm on Urinary Catheter Material. *Antimicrob. Agents Chemother.* **1985**, *27*, 619−624.

(5) Donlan, R. M.; Costerton, J. W. Biofilms: Survival Mechanisms of Clinically Relevant Microorganisms. *Clin. Microbiol. Rev.* **2002**, *15*, 167−193.

(6) McLaughlin-Borlace, L.; Stapleton, F.; Matheson, M.; Dart, J. Bacterial Biofilm on Contact Lenses and Lens Storage Cases in Wearers with Microbial Keratitis. *J. Appl. Microbiol.* **1998**, *84*, 827−838.

(7) Campoccia, D.; Montanaro, L.; Arciola, C. R. The Significance of Infection Related to Orthopedic Devices and Issues of Antibiotic Resistance. *Biomaterials* **2006**, *27*, 2331−2339.

(8) Guaglianone, E.; Cardines, R.; Vuotto, C.; Di Rosa, R.; Babini, V.; Mastrantonio, P.; Donelli, G. Microbial Biofilms Associated with Biliary Stent Clogging. *FEMS Immunol. Med. Microbiol.* **2010**, *59*, 410−420.

(9) Noimark, S.; Dunnill, C. W.; Wilson, M.; Parkin, I. P. The Role of Surfaces in Catheter-associated Infections. *Chem. Soc. Rev.* **2009**, *38*, 3435−3448.

(10) Darouiche, R. O. Treatment of Infections Associated with Surgical Implants. *N. Engl. J. Med.* **2004**, *350*, 1422−1429.

(11) Stewart, P. S.; William Costerton, J. Antibiotic Resistance of Bacteria in Biofilms. *Lancet* **2001**, *358*, 135−138.

(12) Kenawy, E.-R.; Worley, S.; Broughton, R. The Chemistry and Applications of Antimicrobial Polymers: A State-of-the-Art Review. *Biomacromolecules* **2007**, *8*, 1359−1384.

(13) McDonnell, G.; Russell, A. D. Antiseptics and Disinfectants: Activity, Action, and Resistance. *Clin. Microbiol. Rev.* **1999**, *12*, 147−179.

(14) Sharma, V. K.; Yngard, R. A.; Lin, Y. Silver Nanoparticles: Green Synthesis and Their Antimicrobial Activities. *Adv. Colloid Interface Sci.* **2009**, *145*, 83−96.

(15) Onaizi, S. A.; Leong, S. S. Tethering Antimicrobial Peptides: Current Status and Potential Challenges. *Biotechnol. Adv.* **2011**, *29*, 67−74.

(16) Bagheri, M.; Beyermann, M.; Dathe, M. Immobilization Reduces the Activity of Surface-bound Cationic Antimicrobial Peptides with No Influence Upon the Activity Spectrum. *Antimicrob. Agents Chemother.* **2009**, *53*, 1132−1141.

(17) Hancock, R. E.; Sahl, H.-G. Antimicrobial and Host-Defense Peptides as New Anti-infective Therapeutic Strategies. *Nat. Biotechnol.* **2006**, *24*, 1551−1557.

(18) Yeaman, M. R.; Yount, N. Y. Mechanisms of Antimicrobial Peptide Action and Resistance. *Parmacol. Rev.* **2003**, *55*, 27−55.

(19) Hancock, R. E.; Lehrer, R. Cationic Peptides: A New Source of Antibiotics. *Trends Biotechnol.* **1998**, *16*, 82−88.

(20) Jenssen, H.; Hamill, P.; Hancock, R. E. Peptide Antimicrobial Agents. *Clin. Microbiol. Rev.* **2006**, *19*, 491−511.

(21) Gregory, K.; Mello, C. M. Immobilization of Escherichia Coli Cells by Use of the Antimicrobial Peptide Cecropin P1. *Appl. Environ. Microbiol.* **2005**, *71*, 1130−1134.

(22) Uzarski, J. R.; Mello, C. M. Detection and Classification of Related Lipopolysaccharides via a Small Array of Immobilized Antimicrobial Peptides. *Anal. Chem.* **2012**, *84*, 7359−7366.

(23) Uzarski, J. R.; Tannous, A.; Morris, J. R.; Mello, C. M. The Effects of Solution Structure on the Surface Conformation and Orientation of a Cysteine-terminated Antimicrobial Peptide Cecropin P1. *Colloids Surf., B* **2008**, *67*, 157−165.

(24) Zasloff, M. Antimicrobial Peptides of Multicellular Organisms. *Nature* **2002**, *415*, 389−395.

(25) Ge, Y.; MacDonald, D. L.; Holroyd, K. J.; Thornsberry, C.; Wexler, H.; Zasloff, M. In Vitro Antibacterial Properties of Pexiganan, An Analog of Magainin. *Antimicrob. Agents Chemother.* **1999**, *43*, 782−788.

DOI: 10.1021/jp5125487
J. Phys. Chem. C 2015, 119, 7146−7155

(26) Zasloff, M. Magainins, a Class of Antimicrobial Peptides from Xenopus Skin:Isolation, Characterization of Two Active Forms, and Partial cDNA Sequence of a Precursor. *Proc. Natl. Acad. Sci. U. S. A.* **1987**, *84*, 5449−5453.
(27) Ramamoorthy, A.; Thennarasu, S.; Lee, D.-K.; Tan, A.; Maloy, L. Solid-state NMR Investigation of the Membrane-disrupting Mechanism of Antimicrobial Peptides MSI-78 and MSI-594 Derived from Magainin 2 and Melittin. *Biophys. J.* **2006**, *91*, 206−216.
(28) Buer, B. C.; Chugh, J.; Al-Hashimi, H. M.; Marsh, E. N. G. Using Fluorine Nuclear Magnetic Resonance to Probe the Interaction of Membrane-Active Peptides with the Lipid Bilayer. *Biochemistry* **2010**, *49*, 5760−5765.
(29) Brogden, K. A. Antimicrobial Peptides: Pore Formers or Metabolic Inhibitors in Bacteria? *Nat. Rev. Microbiol.* **2005**, *3*, 238−250.
(30) Yang, P.; Ramamoorthy, A.; Chen, Z. Membrane Orientation of MSI-78 Measured by Sum Frequency Generation Vibrational Spectroscopy. *Langmuir* **2011**, *27*, 7760−7767.
(31) Sato, H.; Feix, J. B. Peptide−Membrane Interactions and Mechanisms of Membrane Destruction by Amphipathic α-helical Antimicrobial Peptides. *Biochim. Biophys. Acta, Biomembr.* **2006**, *1758*, 1245−1256.
(32) Lee, D.-K.; Brender, J. R.; Sciacca, M. F.; Krishnamoorthy, J.; Yu, C.; Ramamoorthy, A. Lipid Composition-Dependent Membrane Fragmentation and Pore-Forming Mechanisms of Membrane Disruption by Pexiganan (MSI-78). *Biochemistry* **2013**, *52*, 3254−3263.
(33) Gottler, L. M.; Ramamoorthy, A. Structure, Membrane Orientation, Mechanism, and Function of Pexiganan—A Highly Potent Antimicrobial Peptide Designed from Magainin. *Biochim. Biophys. Acta* **2009**, *1788*, 1680−1686.
(34) Hallock, K. J.; Lee, D.-K.; Ramamoorthy, A. MSI-78, An Analogue of the Magainin Antimicrobial Peptides, Disrupts Lipid Bilayer Structure via Positive Curvature Strain. *Biophys. J.* **2003**, *84*, 3052−3060.
(35) Suzuki, Y.; Buer, B. C.; Al-Hashimi, H. M.; Marsh, E. N. G. Using Fluorine Nuclear Magnetic Resonance to Probe Changes in the Structure and Dynamics of Membrane-active Peptides Interacting with Lipid Bilayers. *Biochemistry* **2011**, *50*, 5979−5987.
(36) Marsh, E. N. G.; Buer, B. C.; Ramamoorthy, A. Fluorine—A New Element in the Design of Membrane-active Peptides. *Mol. Biosyst.* **2009**, *5*, 1143−1147.
(37) Gottler, L. M.; Lee, H. Y.; Shelburne, C. E.; Ramamoorthy, A.; Marsh, E. N. G. Using Fluorous Amino Acids to Modulate the Biological Activity of An Antimicrobial Peptide. *ChemBioChem* **2008**, *9*, 370−373.
(38) Zhu, X.; Suhr, H.; Shen, Y. Surface Vibrational Spectroscopy by Infrared-visible Sum Frequency Generation. *Phys. Rev. B* **1987**, *35*, 3047−3050.
(39) Lambert, A. G.; Davies, P. B.; Neivandt, D. J. Implementing the Theory of Sum Frequency Generation Vibrational Spectroscopy: A Tutorial Review. *Appl. Spectrosc. Rev.* **2005**, *40*, 103−145.
(40) Nguyen, K. T.; Le Clair, S. V.; Ye, S.; Chen, Z. Orientation Determination of Protein Helical Secondary Structures Using Linear and Nonlinear Vibrational Spectroscopy. *J. Phys. Chem. B* **2009**, *113*, 12169−12180.
(41) Liu, Y.; Ogorzalek, T. L.; Yang, P.; Schroeder, M. M.; Marsh, E. N. G.; Chen, Z. Molecular Orientation of Enzymes Attached to Surfaces through Defined Chemical Linkages at the Solid−Liquid Interface. *J. Am. Chem. Soc.* **2013**, *135*, 12660−12669.
(42) Yang, P.; Glukhova, A.; Tesmer, J. J.; Chen, Z. Membrane Orientation and Binding Determinants of G Protein-Coupled Receptor Kinase 5 as Assessed by Combined Vibrational Spectroscopic Studies. *PLoS One* **2013**, *8*, e82072.
(43) Nguyen, K. T.; Le Clair, S. V.; Ye, S.; Chen, Z. Molecular Interactions between Magainin 2 and Model Membranes in situ. *J. Phys. Chem. B* **2009**, *113*, 12358−12363.
(44) Shen, Y. Surface Properties Probed by Second-Harmonic and Sum-Frequency Generation. *Nature* **1989**, *337*, 519−525.
(45) Zhuang, X.; Miranda, P.; Kim, D.; Shen, Y. Mapping Molecular Orientation and Conformation at Interfaces by Surface Nonlinear Optics. *Phys. Rev. B* **1999**, *59*, 12632−12640.
(46) Chen, Z.; Shen, Y.; Somorjai, G. A. Studies of Polymer Surfaces by Sum Frequency Generation Vibrational Spectroscopy. *Annu. Rev. Phys. Chem.* **2002**, *53*, 437−465.
(47) Fu, L.; Liu, J.; Yan, E. C. Chiral Sum Frequency Generation Spectroscopy for Characterizing Protein Secondary Structures at Interfaces. *J. Am. Chem. Soc.* **2011**, *133*, 8094−8097.
(48) Xiao, D.; Fu, L.; Liu, J.; Batista, V. S.; Yan, E. C. Amphiphilic Adsorption of Human Islet Amyloid Polypeptide Aggregates to Lipid/Aqueous Interfaces. *J. Mol. Biol.* **2012**, *421*, 537−547.
(49) Kim, J.; Cremer, P. S. Elucidating Changes in Interfacial Water Structure upon Protein Adsorption. *ChemPhysChem* **2001**, *2*, 543−546.
(50) Kim, G.; Gurau, M.; Kim, J.; Cremer, P. S. Investigations of Lysozyme Adsorption at the Air/Water and Quartz/Water Interfaces by Vibrational Sum Frequency Spectroscopy. *Langmuir* **2002**, *18*, 2807−2811.
(51) Kim, J.; Kim, G.; Cremer, P. S. Investigations of Polyelectrolyte Adsorption at the Solid/liquid Interface by Sum Frequency Spectroscopy: Evidence for Long-Range Macromolecular Alignment at Highly Charged Quartz/Water Interfaces. *J. Am. Chem. Soc.* **2002**, *124*, 8751−8756.
(52) Roy, S.; Covert, P. A.; FitzGerald, W. R.; Hore, D. K. Biomolecular Structure at Solid−Liquid Interfaces As Revealed by Nonlinear Optical Spectroscopy. *Chem. Rev.* **2014**, *114*, 8388−8415.
(53) Kim, J.; Somorjai, G. A. Molecular Packing of Lysozyme, Fibrinogen, and Bovine Serum Albumin on Hydrophilic and Hydrophobic Surfaces Studied by Infrared-Visible Sum Frequency Generation and Fluorescence Microscopy. *J. Am. Chem. Soc.* **2003**, *125*, 3150−3158.
(54) Onorato, R. M.; Yoon, A. P.; Lin, J. T.; Somorjai, G. A. Adsorption of Amino Acids and Dipeptides to the Hydrophobic Polystyrene Interface Studied by SFG and QCM: The Special Case of Phenylalanine. *J. Phys. Chem. C* **2012**, *116*, 9947−9954.
(55) McCrea, K.; Parker, J. S.; Chen, P.; Somorjai, G. Surface Structure Sensitivity of High-pressure CO Dissociation on Pt (557), Pt (100) and Pt (111) Using Sum Frequency Generation Surface Vibrational Spectroscopy. *Surf. Sci.* **2001**, *494*, 238−250.
(56) Lu, X.; Shephard, N.; Han, J.; Xue, G.; Chen, Z. Probing Molecular Structures of Polymer/Metal Interfaces by Sum Frequency Generation Vibrational Spectroscopy. *Macromolecules* **2008**, *41*, 8770−8777.
(57) Lu, X.; Xue, G.; Wang, X.; Han, J.; Han, X.; Hankett, J.; Li, D.; Chen, Z. Directly Probing Molecular Ordering at the Buried Polymer/Metal Interface 2: Using P-Polarized Input Beams. *Macromolecules* **2012**, *45*, 6087−6094.
(58) Ye, S.; Nguyen, K. T.; Boughton, A. P.; Mello, C. M.; Chen, Z. Orientation Difference of Chemically Immobilized and Physically Adsorbed Biological Molecules on Polymers Detected at the Solid/Liquid Interfaces in Situ. *Langmuir* **2009**, *26*, 6471−6477.
(59) Ye, S.; Nguyen, K. T.; Chen, Z. Interactions of Alamethicin with Model Cell Membranes Investigated Using Sum Frequency Generation Vibrational Spectroscopy in Real Time in Situ. *J. Phys. Chem. B* **2010**, *114*, 3334−3340.
(60) Richmond, G. L.; Robinson, J.; Shannon, V. Second Harmonic Generation Studies of Interfacial Structure and Dynamics. *Prog. Surf. Sci.* **1988**, *28*, 1−70.
(61) Yatawara, A. K.; Tiruchinapally, G.; Bordenyuk, A. N.; Andreana, P. R.; Benderskii, A. V. Carbohydrate Surface Attachment Characterized by Sum Frequency Generation Spectroscopy. *Langmuir* **2009**, *25*, 1901−1904.
(62) Wang, J.; Even, M. A.; Chen, X.; Schmaier, A. H.; Waite, J. H.; Chen, Z. Detection of Amide I Signals of Interfacial Proteins in Situ Using SFG. *J. Am. Chem. Soc.* **2003**, *125*, 9914−9915.
(63) Chen, X.; Wang, J.; Sniadecki, J. J.; Even, M. A.; Chen, Z. Probing α-Helical and β-Sheet Structures of Peptides at Solid/liquid Interfaces with SFG. *Langmuir* **2005**, *21*, 2662−2664.

DOI: 10.1021/jp5125487
J. Phys. Chem. C 2015, 119, 7146−7155

(64) Ding, B.; Chen, Z. Molecular Interactions Between Cell Penetrating Peptide Pep-1 and Model Cell Membranes. *J. Phys. Chem. B* **2012**, *116*, 2545−2552.
(65) Wei, S.; Knotts, T. A., IV; Coarse Grain, A. Model for Protein-surface Interactions. *J. Chem. Phys.* **2013**, *139*, 095102.
(66) Karanicolas, J.; Brooks, C. L. Integrating Folding Kinetics and Protein Function: Biphasic Kinetics and Dual Binding Specificity in a WW Domain. *Proc. Natl. Acad. Sci. U. S. A.* **2004**, *101*, 3432−3437.
(67) Karanicolas, J.; Brooks, C. L. The Structural Basis for Biphasic Kinetics in the Folding of the WW Domain from a Formin-binding Protein: Lessons for Protein Design? *Proc. Natl. Acad. Sci. U. S. A.* **2003**, *100*, 3954−3959.
(68) Wei, Y.; Latour, R. A. Benchmark Experimental Data Set and Assessment of Adsorption Free Energy for Peptide− Surface Interactions. *Langmuir* **2009**, *25*, 5637−5646.
(69) Nelson, D. L.; Lehninger, A. L.; Cox, M. M. *Lehninger Principles of Biochemistry*; Macmillan: London, 2008.
(70) Han, X.; Soblosky, L.; Slutsky, M.; Mello, C. M.; Chen, Z. Solvent Effect and Time-Dependent Behavior of C-Terminus-Cysteine-Modified Cecropin P1 Chemically Immobilized on a Polymer Surface. *Langmuir* **2011**, *27*, 7042−7051.
(71) Han, X.; Uzarski, J. R.; Mello, C. M.; Chen, Z. Different Interfacial Behaviors of N-and C-Terminus Cysteine-Modified Cecropin P1 Chemically Immobilized onto Polymer Surface. *Langmuir* **2013**, *29*, 11705−11712.
(72) Han, X.; Liu, Y.; Wu, F.-G.; Jansensky, J.; Kim, T.; Wang, Z.; Brooks, C. L., III; Wu, J.; Xi, C.; Mello, C. M. Different Interfacial Behaviors of Peptides Chemically Immobilized on Surfaces with Different Linker Lengths and via Different Termini. *J. Phys. Chem. B* **2014**, *118*, 2904−2912.
(73) Peschel, A.; Otto, M.; Jack, R. W.; Kalbacher, H.; Jung, G.; Götz, F. Inactivation of the Dlt Operon in Staphylococcus Aureus Confers Sensitivity to Defensins, Protegrins, and Other Antimicrobial Peptides. *J. Biol. Chem.* **1999**, *274*, 8405−8410.

DOI: 10.1021/jp5125487
J. Phys. Chem. C 2015, 119, 7146−7155